Materials Today Bio 23 (2023) 100861

Contents lists available at ScienceDirect

Materials Today Bio

journal homepage: www.journals.elsevier.com/materials-today-bio

Effect of high cyclic hydrostatic pressure on osteogenesis of mesenchymal stem cells cultured in liquefied micro-compartments

Maryam Ghasemzadeh-Hasankolaei [a], Carlos A. Pinto [b], Diana Jesus [a], Jorge A. Saraiva [b], João F. Mano [a,*]

[a] CICECO–Aveiro Institute of Materials, Department of Chemistry, University of Aveiro, 3810-193, Aveiro, Portugal
[b] LAQV-REQUIMTE, Department of Chemistry, University of Aveiro, 3810-193, Aveiro, Portugal

ARTICLE INFO

Keywords:
Mechanical stimulation
Liquefied microcapsules
Hydrostatic pressure
Mesenchymal stem cells
Osteogenic differentiation

ABSTRACT

Bone resident cells are constantly subjected to a range of distinct mechanical loadings, which generates a complex microenvironment. In particular, hydrostatic pressure (HP) has a key impact on modulation of cell function and fate determination. Although HP is a constant mechanical stimulus, its role in regulating the osteogenesis process within a defined 3D microenvironment has not been comprehensively elucidated. Perceiving how environmental factors regulate the differentiation of stem cells is essential for expanding their regenerative potential. Inspired by the mechanical environment of bone, this study attempted to investigate the influence of different ranges of cyclic HP on human adipose-derived mesenchymal stem cells (MSCs) encapsulated within a compartmentalized liquefied microenvironment. Taking advantage of the liquefied environment of microcapsules, MSCs were exposed to cyclic HP of 5 or 50 MPa, 3 times/week at 37 °C. Biological tests using fluorescence staining of F-actin filaments showed a noticeable improvement in cell-cell interactions and cellular network formation of MSCs. These observations were more pronounced in osteogenic (OST) condition, as confirmed by fluorescent staining of vinculin. More interestingly, there was a significant increase in alkaline phosphatase activity of MSCs exposed to 50 MPa magnitude of HP, even in the absence of osteoinductive factors. In addition, a greater staining area of both osteopontin and hydroxyapatite was detected in the 50 MPa/OST group. These findings highlight the benefit of hydrostatic pressure to regulate osteogenesis of MSCs as well as the importance of employing simultaneous biochemical and mechanical stimulation to accelerate the osteogenic potential of MSCs for biomedical purposes.

Credit Author Statement

Maryam Ghasemzadeh-Hasankolaei: Investigation, Methodology, Writing – original draft, Visualization, Carlos A. Pinto: Investigation, Writing – review & editing, Diana Jesus: Investigation, Jorge A. Saraiva: Supervision, Writing – review & editing, João F. Mano: Conceptualization, Supervision, Writing – review & editing, Funding acquisition

1. Introduction

Cells in native tissues reside in a dynamic and complex niche that consists of extracellular matrix (ECM), other cellular populations, as well as various soluble factors (i.e., growth factors and cytokines) [1–3]. Tissue-resident cells are modulated by various biochemical and/or biophysical signals which arise from the cell microenvironment, providing multiple stimulations for cells. The complex cell macro- and microenvironments are involved in the modulation of complex signaling pathways which impact cell adhesion, morphogenesis, proliferation, apoptosis, and differentiation [4–6]. The role of biochemical cues has been intensively investigated by researchers due to their direct effect in triggering biochemical pathways. Growth factors are key biochemical cues that have a fundamental regulatory role in a range of physiological and pathological processes, including tissue maintenance and repair. Soluble growth factors are commonly used either directly by adding to the culture media or indirectly by releasing from a biomaterial carrier [3,7]. Whilst there are numerous literature describing how biochemical factors guide cell behavior *in vitro*, these stimuli are often insufficient for achieving a desirable response, due to the lack of an appropriate mechanical environment. Therefore, not only biochemical factors but also biomechanical signals are essential for controlling cell behavior [7,8].

* Corresponding author.
E-mail address: jmano@ua.pt (J.F. Mano).

https://doi.org/10.1016/j.mtbio.2023.100861
Received 23 February 2023; Received in revised form 4 November 2023; Accepted 9 November 2023
Available online 15 November 2023

For instance, the differentiation of mesenchymal stem cells (MSCs) towards an osteogenic lineage is known to be mechanosensitive *in vitro* [9,10]. Hydrostatic pressure, viscosity, compression and tension, and fluid flow induced shear stress are the main components which define the mechanical environment of bone marrow [11]. Moreover, properties like stiffness and topography are also factors that need to be considered. Some research studies emphasized the importance of substrate topography on differentiation path of different cell types, where this effect can be regulated by shape and size of surface topographical pattern [12,13]. It has been demonstrated that hierarchical topography promoted osteogenic differentiation of human MSCs [12]. Compression and tension also impact proliferation and differentiation of MSCs [14,15]. However, a study which compared cyclic tension and compression reported that tension regulated osteogenic related genes while dynamic compression caused regulation of genes related to chondrogenesis [16]. Moreover, researchers have shown that applying cyclic tensile strain to human MSCs led to osteogenic differentiation without the addition of osteogenic supplements, where a significant increase of BMP-2 expression was observed [17]. Therefore, mechanical cues can be served as an important inducer to control and manipulate cell functions [7,18–22].

Bone is constantly exposed to a range of macro-scale forces which creates a complex mechanical environment. Resident cells including bone marrow MSCs and osteocytes actively sense and accordingly respond to the physical loadings which receive from the surrounding environment. These cells play an important role in various physiological functions such as the maintenance of the skeletal mass and structure [6,23–25]. One of the mechanical stimuli that bone resident cells experience is hydrostatic pressure (HP). In bone, HP exists as a result of gravitational forces and muscle contractions inputs, leading to exert a force by the surrounding liquid to the cells' membrane [26,27]. Externally applied forces have been demonstrated to have a significant impact on cellular function [23,24,28–30]. HP of different values from as small as 10 kPa [24] to as large as 10 MPa [31,32] enhances the differentiation and maturation of MSCs [33,34]. Of particular interest in bone tissue engineering, HP is considered as one of the most important signals in providing suitable biophysical environment for MSCs differentiation. MSCs have been shown to respond to HP *in vitro* at low magnitude, while the level of pressure in bone environment may reach a peak value of 5 MPa *in vivo* [35,36]. Therefore, it would be more physiologically relevant if MSCs are subjected to substantially higher levels of HP, up to the maximum magnitude that cells can tolerate. The pressure up to 100 MPa is called physiological pressure for eukaryotic cells, while the pressure between 100 and 250 MPa is considered as non-physiologic pressure [37]. This means that the effect of the pressure showed different outcomes and it is dependent on the species and on the type of the pressurized cell [37].

Cyclic HP was found to have a positive impact on early osteogenic response of human bone marrow MSCs, which result in upregulation of COX2 and increasing ATP release in a magnitude-dependent manner [24]. It was also shown that cyclic HP was a potent mediator of cytoskeletal reorganization which enhanced the osteogenic responses in MSCs [23]. The intermediate filament (IF) network underwent a breakdown and reorganization with centripetal translocation of IF bundles toward the perinuclear region, which is required for loading-induced MSC osteogenesis [23]. According to the literature, intermittent application of mechanical cues is more beneficial than static loading for boosting bone regeneration [23,25], as dynamic induction preserves the sensitivity of MSCs to the physical stimulations (mechanosensitivity) [25]. Although bone resident cells are constantly exposed to the cyclic mechanical loading of HP and several studies have highlighted its significance, little is known about the influence of this external stimulus in a 3D microenvironment. In 2D environments, physical force applied to cells is in one-direction, while mechanical loading is multidirectional in physiological conditions. Dimensionalities of cell microenvironment changes the mechanical stimulation-induced cell behavior [25]. Therefore, 3D models may offer more physiological environments for mechanotransduction studies. It has been shown that cells behave differently in 2D and 3D environments and a 2D culture does not mimic the natural cellular environment well. For instance, results showed that osteoblastic cells behave differently in 2D and 3D environments not only in static condition, but also in presence of mechanical stimulation [38]. Therefore, more studies are needed to investigate the cell behavior under HP in a controlled 3D environment.

Inspired by the native bone mechanical microenvironment, this work explored the influence of HP on the microtissues developed in liquefied compartments. Initially, various levels of HP (5–250 MPa) were applied to the human adipose-derived MSCs to determine the maximum magnitude of HP that MSCs can withstand. In the last decades, adipose-derived MSCs have emerged as a possible tool in regenerative medicine and cell therapy due to their several advantages including abundance, readily accessible, ease of isolation [39]. Clinical advantages of utilizing adipose-derived MSCs compared to bone marrow-derived MSCs for bone tissue engineering include use of a less invasive method for tissue procurement and the capability to achieve greater numbers of stem cells isolated from the original tissue [40,41]. Moreover, proangiogenic properties of adipose-derived MSCs [39,42] as well as successful culture of them with various biomaterials *in vivo*, both in animal and human models, made them a useful candidate for tissue engineering based therapy [43–46].

According to the results of the first part, two different magnitudes of HP were applied to the adipose-derived MSCs encapsulated in 3D compartmentalized structures. Liquified microcapsules [47–49], already tested *in vivo* [50], have been developed in our group as a versatile platform that can be employed for various applications. By modifying the configuration, this system can be served as a bone marrow model for recapitulation of osteovascular niches [51], a tool for investigating various mechanical cues [22,52], or as microbioreactors inducing different shear stresses [22]. In the proposed system, the encapsulated cells were cultured in contact with surface functionalized microparticles which provided cell attachment sites. This encapsulation system has been shown a great potential to simulate a more close-to-native bone marrow microenvironment, where the biophysical stimulations would create more similarity to the native environment [51]. This is the very first time that the impact of HP has been studied in such a liquified system. We believe that the proposed platform would better reflect the complexity of 3D native tissue microenvironments. We can also propose these liquefied compartments as bioreactors to produce individual microtissues to be employed as units in bottom-up tissue engineering approaches [53] or in disease modelling [54]. Understanding how physical factors regulate the differentiation of MSCs is essential for developing an *in vitro* model for bone regeneration and to unlock MSCs' full regenerative potential. On the other hand, there are not any reports on the effect of large-scale HP. Therefore, this work aims to investigate the influence of high hydrostatic pressure (HHP) on osteogenic differentiation of MSCs.

2. Materials and methods

2.1. Cell culture

Human adipose-derived MSCs were isolated as reported in a previous work in our group [55]. MSCs were cultured in α-MEM (Thermo Fisher Scientific), under a humidified air atmosphere with 5 % CO_2 at 37 °C. α-MEM was supplemented with 10 % heat-inactivated fetal bovine serum (FBS, Thermo Fisher Scientific) and 1 % antibiotic–antimycotic (100x, Gibco, Thermo Fisher Scientific), counted as basal medium (BAS). Medium was changed every three to four days.

2.2. Single cell pressurization

MSCs were detached using 0.05 % w/v trypsin-EDTA (Merck) solution at 37 °C for 5 min. After counting, they were resuspended in BAS

medium and sealed. They were exposed to different levels of HHP ranging between 5 and 250 (5, 10, 35, 50, 100, 150, 200, 250) MPa for a short-term period (10 min). The HP equipment was Unipress U33 (Institute of High-Pressure Physics, Warsaw, Poland) with a pressure vessel of 35 mm inner diameter and 100 mm height surrounded by an external jacket. A thermostatic bath (Huber Compatible Control CC1, New Jersey, USA) was connected to the HP equipment to control the temperature. Metabolic activity of MSCs was quantitatively assessed by MTS colorimetric assay (CellTiter 96 AQueous One Solution Cell Proliferation Assay, Promega), according to the manufacturer's instructions. After the pressurization process, cells were incubated with MTS solution diluted in PBS for 4 h at 37 °C. Then, the absorbance was measured (Abs: 490 nm), using a microplate reader (Microplate Reader Synergy HTX, Biotek, USA). MTS results were normalized by the control group. In the next step, cells were exposed to 50 and 100 MPa for a long-term period (1 h), using the same protocol.

2.3. Bioencapsulation setup

At 90 % confluence, MSCs at passage 5 were detached using 0.05 % w/v trypsin-EDTA (Merck) solution at 37 °C for 5 min. Then, 3×10^6 cells ml^{-1} and 30 mg mL^{-1} surface-functionalized microparticles were resuspended in the 1 % w/v of alginate solution (Alginic acid sodium salt from brown algae, medium viscosity, Sigma-Aldrich) in sodium chloride solution (0.15 M, NaCl, LabChem) buffered with 2-(N-morpholino) ethanesulfonic acid (25 mM, MES, Alfa Aesar) (NaCl/MES). The electrospraying technique was employed to produce alginate microbeads encapsulating MSCs and microparticles in a calcium chloride solution (0.10 M, $CaCl_2$, Merck), as a crosslinking bath (15 min at room temperature at RT). The electrospray parameters were set to 50 mL h^{-1} (flow rate), 22 G (needle), 7 cm (tip to collector), and 10 kV (voltage). Using alginate microbeads as templates, a multilayered membrane made of poly (L-lysine) hydrobromide (PLL, Mw ~ 30,000–70,000, Sigma-Aldrich), chitosan (CHT, NovaMatrix), and alginate polyelectrolytes were produced via layer-by-layer assembly technology (n = 12-layers). All the polyelectrolytes (0.5 mg mL^{-1}) were dissolved in NaCl/MES. After a mild core liquefaction process using EDTA solution (20 mM) at pH 6.7 for 5 min, liquefied microcapsules were cultured in basal (BAS) or osteogenic (OST) media up to 21 days. All solutions were sterilized using a 0.22 μm filter and the entire procedure was performed under sterile conditions. Osteogenic medium was supplemented with dexamethasone (10 nM, ACROS Organics), β-glycerophosphate (10 mM, Merck), and ascorbic acid (50 μg ml^{-1}, Merck).

Surface-functionalized microparticles were produced by emulsion solvent evaporation technique as previously described [47]. Briefly, a 5 % w/v poly-ε-caprolactone solution (Mw 80,000, Sigma-Aldrich) in dichloromethane was added to a stirring 0.5 % w/v polyvinyl alcohol solution (PVA, Mw ~ 30,000–70,000, Sigma-Aldrich), under stirring at RT. After two days, following collection of microparticles with centrifugation (300g, 5 min), they were washed several times with distilled water, and sieved to gain a diameter range of 40–60 μm. Microparticles were dried with absolute ethanol. Afterwards, the surface of microparticles was modified by a plasma treatment technique. For this, the microparticles were placed into a reactor chamber fitted with a radio frequency generator (Plasma System ATTO, Electronic Diener). Using atmospheric gas, a low-pressure glow discharge (30 V and 0.2–0.4 mbar for 15 min) was created at RT. Microparticles were sterilized immediately by UV for 30 min, immersed overnight in an acetic acid solution (20 mm) containing collagen I (10 μg cm^{-2}, rat protein tail, Thermo Fisher Scientific), and then stored in PBS at 4 °C. The zeta potential of the microparticles before and after functionalization process was measured at 25 °C with Zetasizer Nano-ZS (Malvern Instruments Ltd., Royston) at the concentration of 0.5 mg of microparticles/mL in PBS.

2.4. Encapsulated cells pressurization process

Taking advantage of the liquefied core environment of the microcapsules, MSCs were exposed to cyclic HP (6 cycles of 10 min each) at 5 or 50 MPa, at 37 °C for 3 times/week, up to three weeks, using an HP equipment (Unipress U33, Institute of High Pressure Physics, University of Warsaw), using a mixture of propylene glycol:water (60:40 V/V) as pressurization fluid.

The viability of encapsulated cells was investigated through a live/dead fluorescence assay, according to the manufacturer's recommendations (ThermoFisher Scientific) at 7, 14, and 21 days of culture. After washing the samples with PBS, the MSCs were incubated with the kit components for 30 min at 37 °C. Finally, the capsules were analyzed by fluorescence microscopy (Axio Imager 2, Zeiss).

The metabolic activity of cells was evaluated using the MTS colorimetric assay, according to the manufacturer's specifications. Briefly, capsules were washed with PBS and incubated in MTS solution diluted in PBS. Samples were incubated at 37 °C and 5 % CO_2 while protecting from light. After 4 h, the absorbance was measured (Abs: 490 nm), using a microplate reader (Synergy HTX, BioTek). MTS results were normalized by dsDNA quantification values.

For DNA quantification, cell lysis was performed by resuspending the capsules in sterilized ultra-pure water and stored at −80 °C for a minimum period of 24 h. Double-stranded DNA quantification assay was performed using a kit (Quant-iTTM PicoGreen® dsDNA assay kit, Life Technologies), according to the manufacturer's recommendations. Using a microplate reader (Synergy HTX, BioTek), fluorescence was read at an excitation wavelength of 485/20 nm and an emission wavelength of 528/20 nm.

For scanning electron microscopy (SEM) after 21 days of culture, capsules were washed with PBS followed by an incubation of 1 h in 4 % w/v formaldehyde in PBS at RT. Then, the samples were subsequently dehydrated in increasing gradient of ethanol for 15 min at RT, sputtered with carbon, and ultimately visualized (15 kV, S4100, Hitachi).

Evaluation of F-actin filaments was performed by fluorescence phalloidin staining. Capsules were fixed in 4 % w/v formaldehyde (Sigma-Aldrich) diluted in PBS, for 1 h and permeabilized with 0.1 % v/v Triton X-100 (Merck) for 5 min at RT. Afterwards, capsules were incubated in a Flash Phalloidin Red 594 solution (Biolegend, USA) diluted 1:40 in PBS at RT for 1 h. After washing with PBS, a DAPI (1:1000 in PBS, 1 mg ml^{-1}, Thermo Fisher Scientific, USA) solution was used to stain cell nuclei for 15 min at RT. The capsules were visualized by fluorescence microscopy (Axio Imager 2, Zeiss). The cellular network was quantified by measuring the branch length, using image J. Image pre-processing including 'unsharp mask', Enhance Local Contrast (CLAHE), and median filtering were performed to enhance the image quality prior to analysis. For analysis, the images were first converted to binary by thresholding, using ImageJ's default thresholding method, referred to as IsoData. Subsequently, the ImageJ built in 'Skeletonize' feature was applied and finally the average branch length was calculated using the Image J plug-in "Analyze Skeleton 2D/3D".

For the evaluation of focal adhesion points, the capsules were fixed in 4 % w/v formaldehyde for 1 h at RT. Following permeabilization with 0.1 % v/v Triton X-100 (Merck) for 5 min at RT, washing with PBS, and blocking (5 % v/v FBS in PBS) for 1h, samples were incubated with rabbit anti-human vinculin antibody (1:40 in 5 % FBS/PBS, Invitrogen) overnight at 4 °C. Subsequently, capsules were incubated with donkey anti-rabbit AlexaFluor 594 (1:400 in 5 % FBS/PBS, BioLegend) for 1h at RT. Capsules were then stained with Flash Phalloidin Green 488 (1:40 in PBS) for 1 h at RT, and finally with DAPI (1:1000 in PBS) for 15 min at RT.

For osteopontin staining, fixed samples were first stained with mouse anti-human osteopontin (1:100 in 5 % FBS/PBS, Biolegend) and anti-mouse Alexa Fluor 647 (1:400 in 5 % FBS/PBS, ThermoFisher Scientific). Then, capsules were incubated with DAPI solution for nuclei visualization (1:1000 in PBS) for 15 min at RT.

The *in vitro* mineralization of capsules was accessed using Osteo-Image™ Mineralization Assay kit (Lonza) according to the manufacturer's instructions. Then capsules were counterstained with DAPI (1:1000 in PBS) for 15 min, RT.

The alkaline phosphatase (ALP) activity was determined by the amount of *p*-nitrophenol. Briefly, 0.2 % w/v of substrate solution (pH 9.8) was prepared by dissolving 4-nitrophenylphosphate disodium salt hexahydrate (Sigma-Aldrich) in 1 M diethanolamine (Sigma-Aldrich). 20 μL of each sample was mixed with the prepared substrate solution (60 μL). After 4 h at 37 °C in dark, the reaction was stopped with 80 μL of NaOH (2 M) including EDTA (0.2 mM). A standard curve with a range of concentrations was used as a reference by diluting 4-nitrophenol solution (10 mM, Sigma-Aldrich) in the stop solution. Lastly, the enzyme activity was measured at 405 nm using a microplate reader (Synergy HTX, BioTek).

2.5. Statistical analysis

Statistical analysis was performed using two-way analysis of variance (ANOVA) with Tukey's post-hoc test to compare more than two groups, and two-tailed unpaired *t*-test to compare two groups. The branch length was analyzed by one-way ANOVA analysis using Tukey's multiple comparisons test (GraphPad Prism 6.0). All assays were carried out at least in three replicates for each condition.

3. Results and discussions

3.1. The effect of different magnitudes of high hydrostatic pressure (HHP) on viability of cells

To investigate the effect of HHP on cellular viability, single cell suspensions were exposed to different levels of HHP ranging between 5 and 250 MPa for a short-term period of 10 min (Fig. 1. A). After 24 h, morphological analysis proved that cells which were under the HHP between 5 and 100 MPa were fully attached and showed a normal morphology after pressurization (Fig. 1. B), indicating that the selected pressure levels did not impact the cellular adhesive properties. Moreover, the quantitative evaluation of the cell's viability immediately after pressurization process revealed that cells subjected to HHP of 5–100 MPa showed a high rate of metabolic activity (Fig. 1. C). There was not any significant difference in metabolic activity of cells which were exposed to HHP between 5 and 100 MPa, which confirmed the morphological observations. However, despite showing high metabolic activity in 100 MPa group, morphological analysis after 24 h revealed the presence of some clusters of cells (arrows) which exhibited a rounded morphology. On the other hand, analyzing both tests demonstrated that HHP at the magnitude of 150, 200, and 250 MPa was extremely lethal to the cells, where a significant difference in metabolic activity and a round shape morphology were observed. In line with our results, it was reported that cells (NIH/3T3, smooth muscle, and endothelial cells) exposed to the pressure above 200 MPa, showed a round shape morphology and did not adhere to the culture dish even after 24 h [56].

According to the earlier results, 50 and 100 MPa were selected for further examination, in which cells were subjected to 50 or 100 MPa HHP for a long-term period (1 h). Morphological investigation after 24 h showed that the exposure of MSCs to the 100 MPa pressure caused severe morphological alteration which indicates cell damage (Fig. 1. C), while cells exposed to 50 MPa showed a normal morphology. On the other hand, metabolic activity analysis showed that although cells after exposure to 100 MPa showed lower metabolic activity compared to 50 MPa, the differences were not significant (Fig. 1. D). These observations

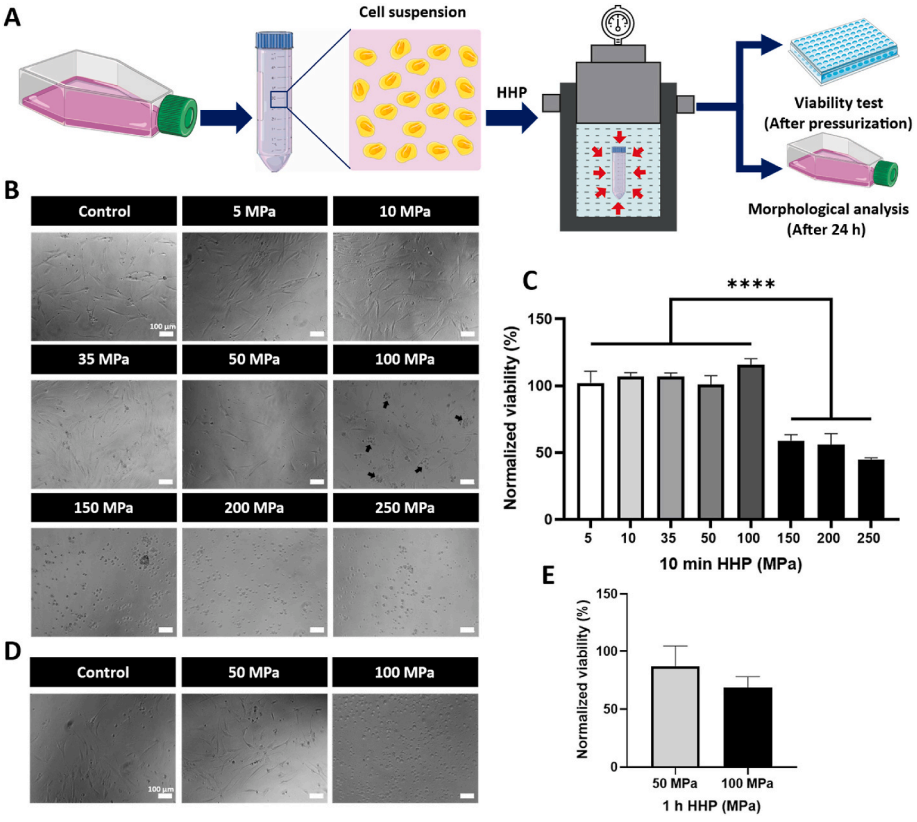

Fig. 1. Effect of different magnitudes of high hydrostatic pressure (HHP) on mesenchymal stem cells (MSCs). A) Schematic description of the pressurization process. B) Morphological observation of MSCs 24 h after being exposed to different HHP levels for 10 min, scale bar = 100 μm. C) Metabolic activity of MSCs immediately after 10 min HHP exposure. D) Morphological analysis of MSCs 24 h after being subjected to 50 or 100 MPa HHP for 1h, scale bar = 100 μm. E) Metabolic activity of MSCs immediately after 1h HHP exposure of 50 and 100 MPa.

could be attributed to the timing of the analyses. The metabolic activity assessment was performed immediately after the pressurization process, while morphological analysis was conducted after 24 h. This suggests that although cells were metabolically active immediately post HHP exposure, they appeared to undergo sever cell death within the following 24 h. In coordinate with our observation, it has been reported that apoptotic cells started to be noticed 8 h after human lymphoblasts were exposed to 100 MPa for 30 min [57]. Although, HHP lower than 100 MPa was considered as bearable HHP for eukaryotic cells [37], comparing the results of the short-term and long-term exposure of 100 MPa showed that cellular response depends on the duration of HHP exposure. Therefore, it is important to note that the severity of cell death is dependent on the cell type sensitivity, magnitude, and duration of exposure to HHP [58]. For example, it was shown that exposure of human dermal fibroblast cell line in suspension culture to HHP at 50 MPa for ≥36 h, induced fibroblast cell death via apoptosis [59].

3.2. Encapsulation of MSCs

Liquified microcapsules encapsulating MSCs and microparticles were successfully produced based on a method previously described by the authors [47] (Fig. 2. A1). Light microscopy of microcapsules demonstrated that they kept their round-shape morphology even after the liquefaction step (Fig. 2. A2). Fig. 2. A3 shows the microparticles visualized by SEM microscopy. Zeta potential measurements of microparticles before (around −10.3 mV) and after (around −5.28 mV) functionalization revealed that microparticles became less negative after functionalization process (Fig. 2. A4). This shift in zeta potential can indicate that the functionalization process was successful. Analysis of light microscopy images of microcapsules using image J showed that microcapsules presented an average diameter of 724 ± 51 μm after the liquefaction process (n = 80) (Fig. 2. A5). These results highlight the possibility of achieving good control over size and shape of the microcapsules using electrospraying technique. Live/dead fluorescence assay showed that MSCs presented a high level of viability after the encapsulation (Fig. 2. A6). The fraction of viable cells was approximately 80 %, by counting the live and dead cells using image J (Fig. 2. A7). The observed high viability is consistent with previous studies which is due to the mild encapsulation process [22,47–49,52,60].

Fig. 2. B represents the pressurization protocol of the microcapsules cultured with or without chemical induction (OST or BAS, respectively). Microcapsules were exposed to the intermittent HHP at pressure magnitudes of 5 or 50 MPa for three weeks.

3.3. Viability of MSCs after exposure to 1 h intermittent HHP over time

Three times a week, the encapsulated cells cultured with or without osteogenic induction were exposed to the intermittent HHP (6 cycle of 10 min) up to 21 days (Fig. 2. B) at 37 °C, under pressures of 5 or 50 MPa. Over the three weeks pressurization process, the membrane of microcapsules was examined using light microscopy to detect any visible damage or rupture that could lead to the leakage of cells and microparticles. Results showed that HHP did not cause any damage to the microcapsules (Fig. S1). The observed high resistance of

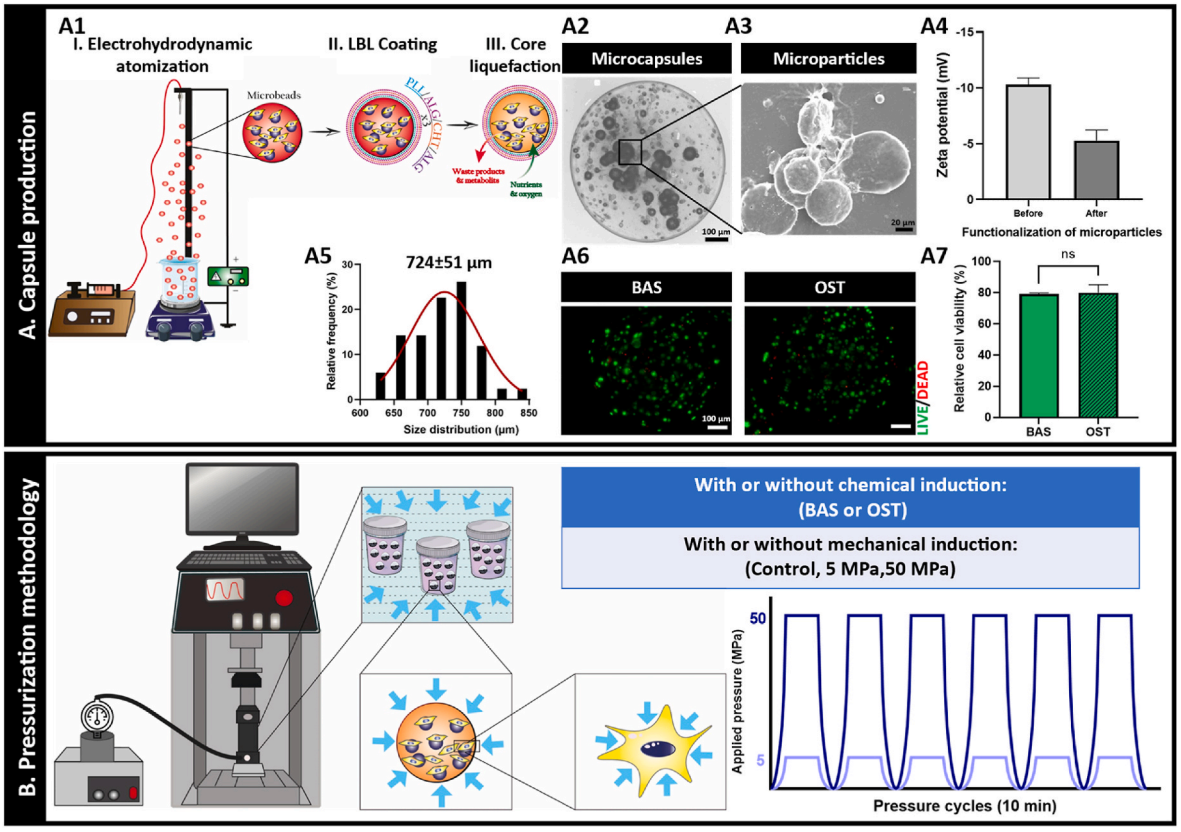

Fig. 2. A) The production process of microcapsules. A1) Schematic illustration of the fabrication process of the liquified multilayered capsules. A solution of alginate containing cells and microparticles was electrosprayed into a calcium chloride bath to produce microbeads. Using the Layer-by-Layer (LbL) technique, a multilayered membrane of capsules is formed around the microbeads. Subsequently, the core liquefaction process is carried out using ethylenediaminetetraacetic acid (EDTA) to produce liquefied microcapsules. A2) Bright field image of a capsule containing MSCs and microparticles, scale bar = 100 μm. A3) SEM image of microparticles used within the microcapsules as cell attachment sites, scale bar = 20 μm. A4) Zeta potential (mV) of microparticles before and after functionalization measured in PBS. A5) Histogram of the size of microcapsules after liquefaction with EDTA (n = 80). A6) Live–dead fluorescence assay of microcapsules and A7) relative cell viability evaluated by the live–dead cell staining, scale bar = 100 μm. B) Schematic representation of pressurization of microcapsules during three-week culture. Microcapsules cultured with or without chemical induction, osteogenic (OST) or basal (BAS), were exposed to different magnitude (5 or 50 MPa) of intermittent HHP.

microcapsules makes them an ideal platform for a variety of biomechanical investigations. Consistent with our findings, high mechanical resistance of these liquefied micro-sized capsules was previously reported by performing rotational mechanical stress at 15000 g [22]. To evaluate whether HHP resulted in any severe cell damage during this period, cells were monitored weakly by live-dead staining and metabolic activity tests. Live-dead fluorescence assay showed that the majority of encapsulated cells stayed viable during the three-weeks culture in all conditions (Fig. 3. A, Fig. S2). Interestingly, the metabolic activity of cells, measured by MTS assay and normalized by the total DNA content, demonstrated an increase over time (Fig. 3. B). Therefore, the chosen pressurization protocol had no cytotoxic effects on encapsulated cells. Moreover, the increased metabolic activity of encapsulated cells over time confirms that the liquified environment and the semipermeable membrane of capsules guaranteed the high diffusion of essential factors. These observations are in line with previous studies which showed high rate of viability in liquefied system [47–49,52,60]. It has been reported that oxygen and glucose can freely pass through the semipermeable membrane [61,62]. Microparticles, which are one of the key components of the system, also had an important role in the high cellular viability by providing cell attachment sites for the encapsulated cells. A few studies have reported the effect of cyclic pressure at different magnitudes on the viability of cells. In one study, cells cultivated in alginate beads were treated with cyclic HP at 5 MPa 4 h/day up to 4 weeks. Results showed that after 4 weeks of culture, not only HP did not cause any cell death but also it promoted cell proliferation, which was confirmed by quantifying the DNA content [63]. In another study, it was demonstrated that application of 2 MPa cyclic HP stimulation for a duration of 4 h per day, for 7 consecutive days did not cause any detrimental effect on viability of MSCs [64]. These reports are in accordance with our observation of increased metabolic activity over time.

3.4. Evaluation of cellular response to the intermittent HHP

To investigate the morphological cell response to the external force, we performed fluorescent staining of F-actin filaments with phalloidin, SEM images analysis, and vinculin fluorescence staining. The F-actin cytoskeleton staining showed that HHP promoted increased cell spreading (Fig. 4. A). This effect was more noticeable in OST medium where more elongated cells were observed. In contrast, cells in both control groups were found to have a more rounded morphology. A possible explanation for this observation is that once cells are stimulated by external signals, integrins transmit the external mechanical forces to the cytoskeleton, therefore modulating the mechanical behavior of the skeleton [65]. Thus, HHP modifies the thermodynamics of the assembly of cytoskeletal proteins, forcing these proteins to depolymerize [66]. In accordance with the present results, previous studies demonstrated that exposure of MSCs to HP stimulation led to distinct remodeling of cytoskeletal elements [23,67]. In another study, mouse embryonic fibroblasts (MEFs) were analyzed for genes related to the actin filament, just after 10 min application of hydrostatic pressure (15, 30, 60, and 90 MPa) [68], with the results showing that despite changes in cell morphology, the expression of genes related to actin filament did not show any

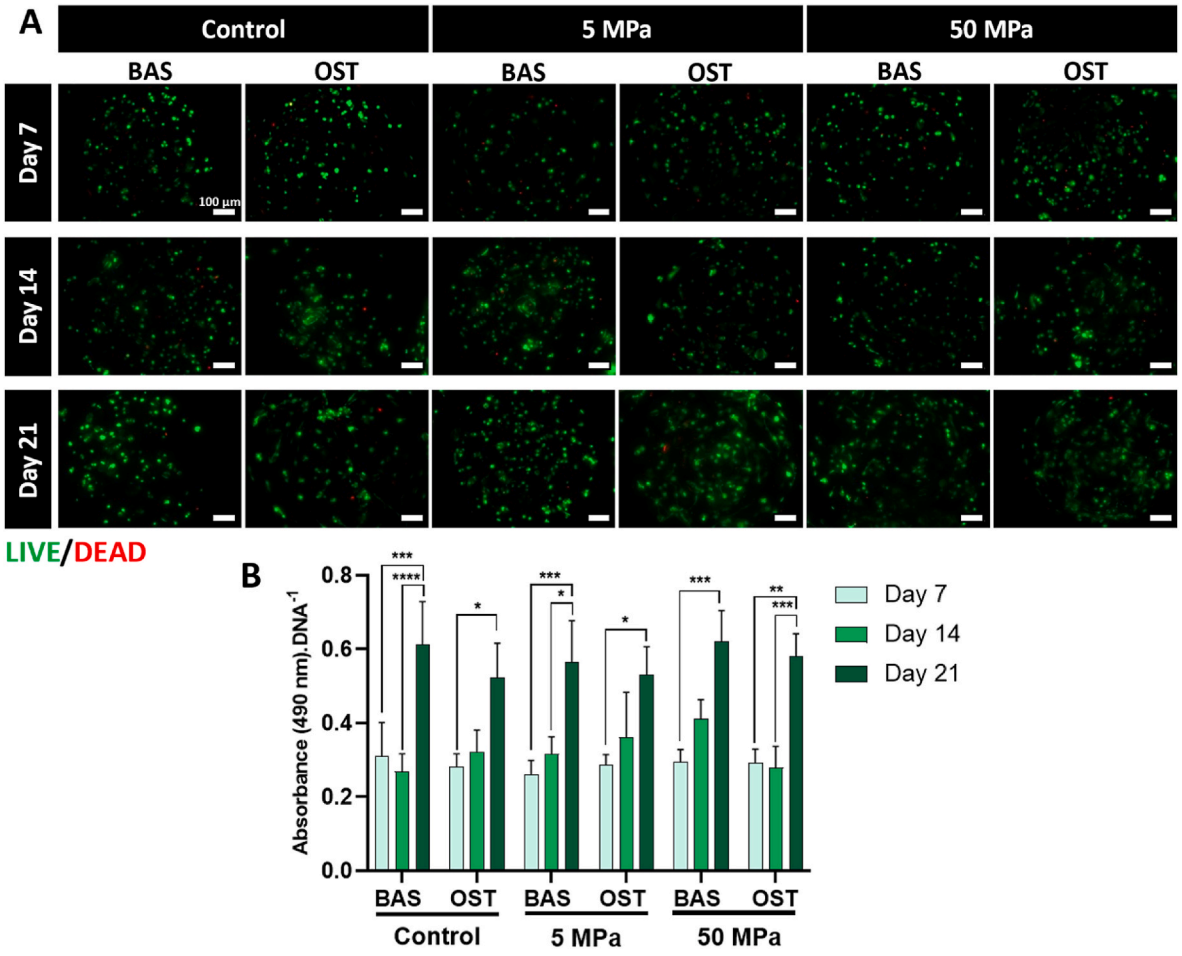

Fig. 3. Effect of different magnitudes of HHP on the viability of MSCs encapsulated within the liquefied capsules. A) Live–dead fluorescence assay of MSCs cultured up to three weeks in basal (BAS) or osteogenic (OST) medium, scale bar = 100 µm. B) Metabolic activity normalized by the total DNA content at 7, 14, and 21 days of culture. *, **, ***, and **** indicates statistical significance with $p < 0.05$, $p < 0.01$, $p < 0.001$, and $p < 0.0001$, respectively.

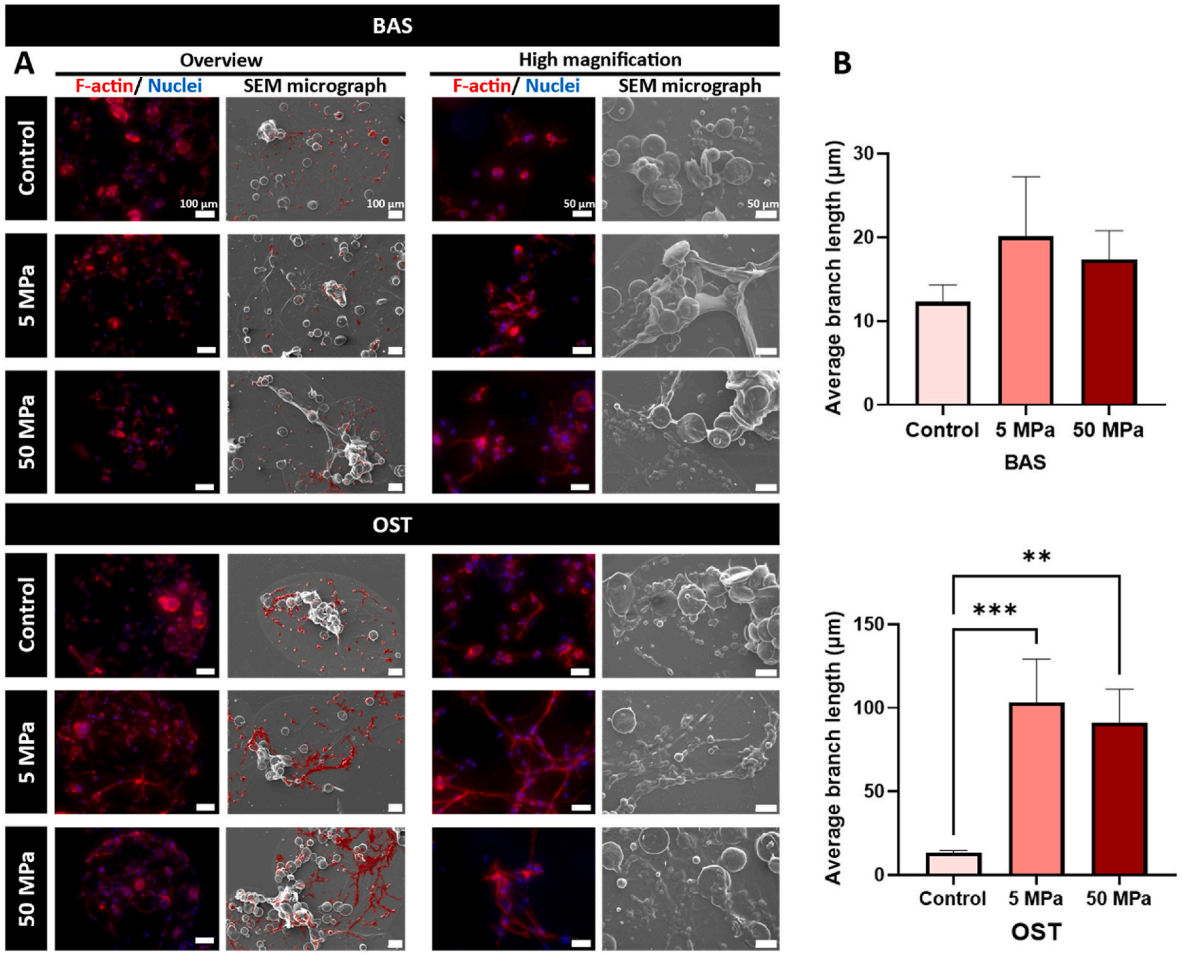

Fig. 4. A) Overview and high magnification of cells inside the microcapsules. Fluorescence images of F-actin (red), and nucleus (blue) staining and SEM micrograph of MSCs (the cellular network colored in red), scale bars are 100 µm and 50 µm, respectively. Nuclei were stained with DAPI, actin was stained with phalloidin. B) Quantification of the cellular network by the measurement of the branch length, using image J. ** and *** indicates statistical significance with $p < 0.01$ and $p < 0.001$, respectively.

significant changes [68]. Such contradictory findings may be due to the different duration of the HP application, which seems that was not enough for MEFs to respond to the stimulation.

Not only the cellular morphology underwent some changes, but also the cellular organization pattern was influenced by HHP (Fig. 4. A). Actin filament staining showed that a considerable number of cells connected to each other and formed a branched network. This allowed cells to have more physical contact and expanded the area of cell–cell interactions. The quantification of the branch length showed that exposure of cells to HHP resulted in an increase in the average length of the branches, more significant in osteogenic medium (Fig. 4. B). The observed results were corroborated by SEM images analysis, where more cellular networks were visible in the microcapsules exposed to HHP (Fig. 4. A). Furthermore, more ECM production was observed in the pressurized groups, to a greater extent noticeable in OST, in comparison to the control groups (Fig. 4. A). These observations are in accordance with other studies reporting that dynamic mechanical stimulation of both human bone marrow- and adipose tissue-derived MSCs enhanced the synthesis of osteogenic matrix components [52,69]. Moreover, chondrocytes are shown to increase production of ECM in response to dynamic hydrostatic pressure [31,70,71]. Furthermore, we explored this phenomenon in-depth, by studying vinculin staining. Vinculin is a cytoskeletal protein associated with cell-cell and cell-matrix junctions, which promotes cell spreading by stabilizing focal adhesions and regulates the interaction between talins and the actin cytoskeleton under high tension conditions [72,73]. Results showed that cells in response to the mechanical stimulation expressed more vinculin, more significant in OST medium (Fig. 5). Most importantly, it was observed that in both 5 and 50 MPa/OST conditions vinculin was expressed more in cell-cell contact (visible in Fig. 5, MPa/OST and Fig. S3 A, video S3 B) and cell-microparticles areas (visible in Fig 5, 50 MPa, OST and Fig. S3 C). In general, the results shown in Figs. 4 and 5 demonstrated that the encapsulated cells could build their own network with the help of microparticles. As seen in Fig. S4, MSCs in all tested groups showed good attachment to the microparticles. Only in the pressurized groups with the osteogenic induction, the branched network of cells was observed. To the best of our knowledge, this is the first time that the development of the branched network in response to the HHP has been reported. This observation is probably due to the uniqueness of the encapsulation system which allows cells to build their own 3D structures.

3.5. *Evaluation of osteogenic differentiation of encapsulated cells in response to intermittent HHP*

To evaluate osteogenic differentiation, the expression of osteopontin (OPN) was analyzed qualitatively by immunofluorescence assay (Fig. 6. A). OPN is a marker expressed during the osteogenic differentiation process of MSCs. OPN interacts with integrin and helps bone cells to adhere to the mineral matrix [74,75]. Results showed that OPN was expressed in osteogenic conditions, with the major expression in the 50 MPa group. Immunofluorescence analysis of collagen I (COL I) on day 14 as well as osteocalcin (OCN) on day 21 showed higher expression of

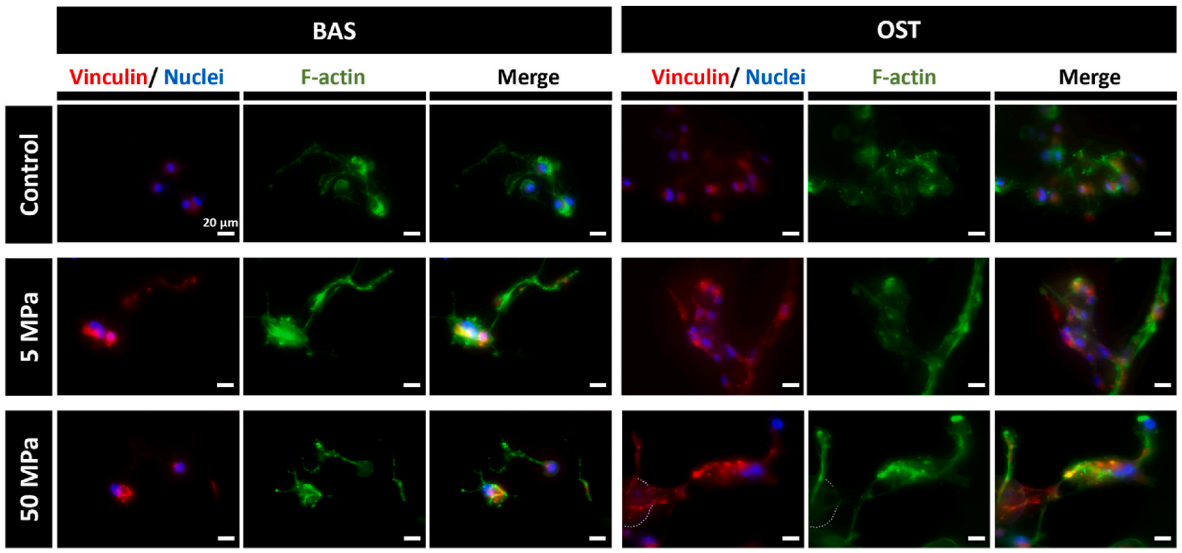

Fig. 5. Fluorescence images of F-actin (green), vinculin (red), and nucleus (blue) staining of MSCs. High expression of vinculin in cell-cell contacts (5 MPa/OST) or cell-microparticles (50 MPa/OST) areas is more noticeable, Scale bar = 20 µm.

these markers in pressurized group (50 MPa), compared to the control group, in both BAS and OST media (Fig. S5. A and B).

Moreover, SEM micrographs showed the presence of different sizes of some structures, more noticeable in pressurized groups (Fig. 6. B). Evidence based on shape and size of these structures suggests that they are probably extracellular vesicles. Extracellular vesicles are bud from the plasma membrane, their diameter varying from nm to µm releasing by many cell types, which have an important role as mediators of cell-to-cell communication. They assist as a vehicle for transmission of proteins and messenger RNA and microRNA to other cells, which changes the gene expression, proliferation, and differentiation of the recipient cells [76]. The presence of several extracellular vesicles can indicate active protein synthesis and secretion [77]. Moreover, there are reports suggesting a relation between the role of extracellular vesicles and bone mineral formation [78,79]. Interestingly, we observed considerably more of these extracellular-vesicle-like-structures in 50 MPa groups. This observation is in line with another study which showed that application of HP increased the extracellular vesicles production of human bone marrow MSCs during chondrogenic differentiation [80].

The differentiation of cells into osteoblasts is characterized by the presence of mineralized hydroxyapatite (HA) nodules. The development of HA in the 3D micro compartments was specifically explored to confirm bone mineralization (Fig. 6. C). Interestingly, considerably greater amount of HA staining was observed in cells cultured under pressurized conditions, even in the absence of OST factors. This finding is consistent with the presence of more extracellular-vesicle-like-structures observed in SEM micrographs (Fig. 6. B). In fact, it has been reported that extracellular vesicles are also located at the sites of the ECM where mineralization would commence [78].

Finally, the osteogenic differentiation was assessed by ALP activity (Fig. 6. D), a marker highly correlated with active bone formation [81]. During 21 days of culture, an increase in ALP activity has been observed in all condition tested, more noticeable in the presence of OST induction. Remarkably, the results showed a significant increase in ALP activity in the 50 MPa condition, compared to the control group, even in the absence of OST induction. In contrary, a reduction of alkaline phosphatase activity in the media of MSCs exposed to 10 MPa of cyclic HP, in the presence of either 1 or 10 ng mL^{-1} of TGF-b3 was reported [82]. Such contradictory effect may be due to the use of TGF-b3, which could induce different signaling pathways.

Taken together, our study demonstrated that cyclic HHP promoted cell-cell contacts and enhanced cellular network. More ECM secretion was also observed in the pressurized groups. Furthermore, higher expression of vinculin confirmed the increased cell-cell interactions. These observations were more significant in the presence of osteoinductive factors. More importantly, analyzing the osteogenic differentiation of MSCs confirmed that cells exposed to the cyclic HHP and cultured in OST medium expressed higher OPN marker. Moreover, the presence of more extracellular-vesicle-like-structures, as well as higher staining of HA, also confirmed the previous results. Most noticeably, ALP activity at 50 MPa was significantly higher than that observed for the control group, even when soluble osteogenic factors were not introduced to the culture. Altogether, these data indicate that cyclic HHP is beneficial for osteogenic differentiation in our bioengineered compartments. This phenomenon is more significant at higher magnitude and in the presence of osteogenic factors. In line with our observations, another study reported that HP promoted osteogenesis [83]. Results showed that 279 kPa of cyclic HP led to enhanced calcium deposition in rat bone marrow derived MSCs which were co-cultured with human umbilical vein endothelial cells (HUVECs) on a porous scaffold [83].

Our results indicate that cytoskeletal remodeling, cell-cell communication, and osteogenic differentiation are interrelated, where more osteogenic differentiation was observed when cells had more elongated morphology, and significantly higher interactions compared to the control group. According to the literature, and in match with our observation, it was reported that cyclic HP is a potent mediator of cytoskeletal reorganization and osteogenic differentiation of MSCs [23]. It was shown that intermediate filament remodeling is essential for loading induced MSC osteogenic differentiation. In addition, another study proved that cell–cell interaction plays an important role in osteogenic differentiation of MSCs [84]. Using micropatterned surfaces, it was reported that MSCs with more interaction partners showed a significantly higher level of osteogenic commitment [84].

On the other hand, while there was no significant difference in ALP activity of MSCs between the 5 MPa groups and the control groups, high cell-cell interactions, high expression of vinculin and OPN, and higher staining of HA were detected. These observations indicate that although osteogenic differentiation was promoted, the mechanical stimulation was not sufficient for the fully differentiation of MSCs. One possible explanation for this effect could be that MSCs respond to the cyclic HP according to the magnitude of pressure. This is consistent with a previous study which reported that cyclic HP stimulated osteogenic response of MSCs in a magnitude- and frequency dependent manner, by applying different magnitudes of cyclic HP to human bone marrow MSCs

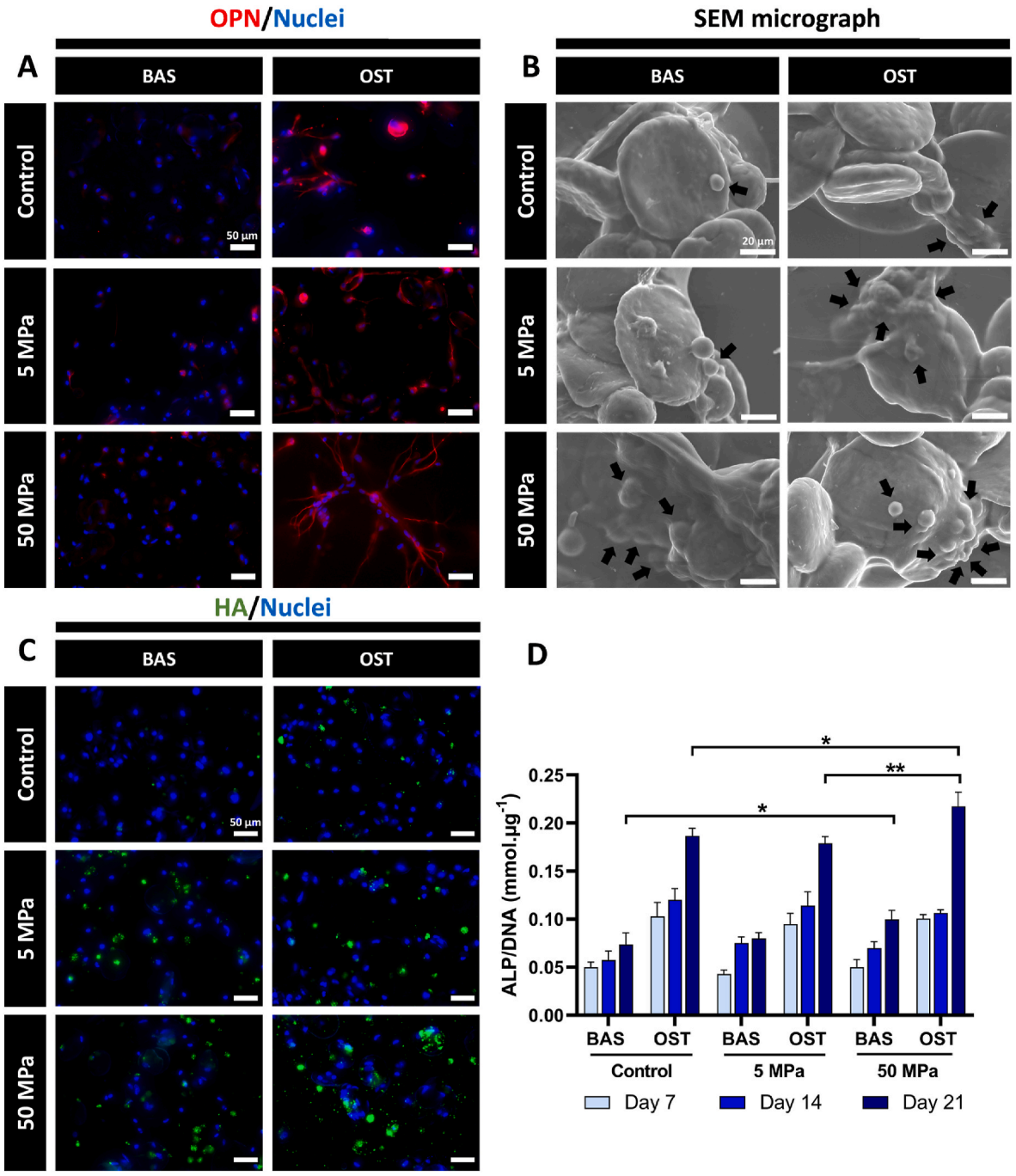

Fig. 6. A) Osteopontin (OPN) staining (red) of MSCs and nuclei (blue). Scale bar = 50 µm B) SEM micrograph of extracellular-vesicle-like-structures (black arrows) in different conditions. Scale bar = 20 µm. C) Fluorescence staining of hydroxyapatite (HA) in green and nuclei in blue. 5 and 50 MPa/OST demonstrated higher HA content. Scale bar = 50 µm. D) ALP activity of MSCs in BAS or OST media under the cyclic HHP condition. * and ** indicates statistical significance with $p < 0.05$ and $p < 0.01$, respectively.

cultured on fibronectin coated glass slide [24].

Finally, we have found that the highest osteogenic differentiation level observed when both chemical (osteogenic medium) and mechanical (HHP) cues were applied simultaneously. The combinatory effect of different stimulations was reported in other studies [85–87]. One study has shown that the combination of shear stress and adhesion morphology stimulations led to the maximum expression level of osteogenic markers including *ALP*, *osteocalcin*, and *collagen type I* [85]. In another work, it was reported that combining fluid shear stress with the presence of bone-like extracellular matrix synergistically improved osteogenesis of rat MSCs [86]. More recently, it has been demonstrated that using both chemical (osteogenic medium) and mechanical (micro-topographically patterned surface) factors simultaneously, enhanced osteogenic differentiation of human MSCs [87]. This phenomenon may be due to the fact that using osteogenic biochemical induction would increase the mechanical sensitivity of MSCs and modulate the mechanical-induced osteogenic response [87,88]. Together, this part of the study underlines the relevance of combining chemical and physical stimulations to effectively regulate the differentiation process.

4. Conclusion

Overall, this study demonstrated that the proposed liquefied encapsulation system holds great promise as an effective platform for investigating the impact of various magnitudes of HP in a variety of biological responses, including stem cells differentiation. Our study emphasizes the importance of HP to fully mimic the native cell mechanical microenvironment. Moreover, it was revealed that the beneficial effect of HP in osteogenic differentiation process is magnitude dependent. Finally, our results shed light on the importance of applying both biochemical and mechanical cues simultaneously to enhance differentiation effectively and efficiently for biomedical purposes. We conclude that the bioengineered microcapsules are quite versatile platforms to provide microtissues in distinct conditions, including under controlled HP. Such compartments are easily handled and could be used as units in a variety of biotechnological applications and to be assembled to engineer larger tissues for therapies or disease models. To unlock the full potential of this technology, further studies are required to explore the impact of HHP on differentiation of other tissues like cartilage. Moreover, to enhance the capabilities of the platform we propose to integrate additional features alongside HHP, such as introducing other mechanical cues (modifying microparticle properties like stiffness). Finally, we envisage testing this platform for bioprinting of anatomically shaped structures.

Declaration of competing interest

The authors declare that they have no known competing financial interests or personal relationships that could have appeared to influence the work reported in this paper.

Data availability

Data will be made available on request.

Acknowledgements

The authors acknowledge support of the doctoral grant (SFRH/BD/147418/2019), the FCT project TETRISSUE (PTDC/BTM-MAT/3201/2020), the European Research Council REBORN (ERC-2021-AdG883370), and the project CICECO-Aveiro Institute of Materials, UIDB/50011/2020, UIDP/50011/2020 & LA/P/0006/2020, financed by national funds through the FCT/MCTES (PIDDAC) and LAQV Research Unit (UIDB/50006/2020 and UIDP/50006/2020). Dr. Sónia G. Patrício is acknowledged for her support in the SEM acquisition.

Appendix A. Supplementary data

Supplementary data to this article can be found online at https://doi.org/10.1016/j.mtbio.2023.100861.

References

[1] W. Li, Z. Yan, J. Ren, X. Qu, Manipulating cell fate: dynamic control of cell behaviors on functional platforms, Chem. Soc. Rev. 47 (23) (2018) 8639–8684, https://doi.org/10.1039/C8CS00053K.
[2] C. Zheng, J. Chen, S. Liu, Y. Jin, Stem cell-based bone and dental regeneration: a view of microenvironmental modulation, Int. J. Oral Sci. 11 (3) (2019) 23, https://doi.org/10.1038/s41368-019-0060-3.
[3] A. Cipitria, M. Salmeron-Sanchez, Mechanotransduction and growth factor signalling to engineer cellular microenvironments, Adv. Healthcare Mater. 6 (15) (2017), 1700052, https://doi.org/10.1002/adhm.201700052.
[4] J. Nicolas, S. Magli, L. Rabbachin, S. Sampaolesi, F. Nicotra, L. Russo, 3D extracellular matrix mimics: fundamental concepts and role of materials chemistry to influence stem cell fate, Biomacromolecules 21 (6) (2020) 1968–1994, https://doi.org/10.1021/acs.biomac.0c00045.
[5] Y. Ma, T. Han, Q. Yang, J. Wang, B. Feng, Y. Jia, Z. Wei, F. Xu, Viscoelastic cell microenvironment: hydrogel-based strategy for recapitulating dynamic ECM mechanics, Adv. Funct. Mater. 31 (24) (2021), 2100848, https://doi.org/10.1002/adfm.202100848.
[6] S. Liu, R. Tao, M. Wang, J. Tian, G.M. Genin, T.J. Lu, F. Xu, Regulation of cell behavior by hydrostatic pressure, Appl. Mech. Rev. 71 (4) (2019), https://doi.org/10.1115/1.4043947.
[7] S. Vermeulen, Z.T. Birgani, P. Habibovic, Biomaterial-induced pathway modulation for bone regeneration, Biomaterials (2022), 121431, https://doi.org/10.1016/j.biomaterials.2022.121431.
[8] D. Jesus, A.R. Pinho, M.C. Gomes, C.S. Oliveira, J.F. Mano, Emerging modulators for osteogenic differentiation: a combination of chemical and topographical cues for bone microenvironment engineering, Soft Mater. 18 (16) (2022) 3107–3119, https://doi.org/10.1039/D2SM00009A.
[9] T. Wu, F. Yin, N. Wang, X. Ma, C. Jiang, L. Zhou, Y. Zong, H. Shan, W. Xia, Y. Lin, Involvement of mechanosensitive ion channels in the effects of mechanical stretch induces osteogenic differentiation in mouse bone marrow mesenchymal stem cells, J. Cell. Physiol. 236 (1) (2021) 284–293, https://doi.org/10.1002/jcp.29841.
[10] A.J. Engler, S. Sen, H.L. Sweeney, D.E. Discher, Matrix elasticity directs stem cell lineage specification, Cell 126 (4) (2006) 677–689, https://doi.org/10.1016/j.cell.2006.06.044.
[11] U.A. Gurkan, O. Akkus, The mechanical environment of bone marrow: a review, Ann. Biomed. Eng. 36 (12) (2008) 1978–1991, https://doi.org/10.1007/s10439-008-9577-x.
[12] L. Yang, L. Ge, Q. Zhou, T. Mokabber, Y. Pei, R. Bron, P. van Rijn, Biomimetic multiscale hierarchical topography enhances osteogenic differentiation of human mesenchymal stem cells, Adv. Mater. Interfac. 7 (14) (2020), 2000385, https://doi.org/10.1002/admi.202000385.
[13] E.H. Ahn, Y. Kim, S.S. An, J. Afzal, S. Lee, M. Kwak, K.-Y. Suh, D.-H. Kim, A. Levchenko, Spatial control of adult stem cell fate using nanotopographic cues, Biomaterials 35 (8) (2014) 2401–2410, https://doi.org/10.1016/j.biomaterials.2013.11.037.
[14] H. Liu, Z. Tian, S. Liu, W. Yang, A. Qian, L. Hu, Z. Wu, Mechanobiology of bone marrow mesenchymal stem cells (BM-MSCs), Bone Cell Biomechanics, Mechanobiology and Bone Diseases, Elsevier 2024, pp. 97-124, https://doi.org/10.1016/B978-0-323-96123-3.00003-8..
[15] A.J. Steward, D.J. Kelly, Mechanical regulation of mesenchymal stem cell differentiation, J. Anat. 227 (6) (2015) 717–731, https://doi.org/10.1111/joa.12243.
[16] A.K. Haudenschild, A.H. Hsieh, S. Kapila, J.C. Lotz, Pressure and distortion regulate human mesenchymal stem cell gene expression, Ann. Biomed. Eng. 37 (2009) 492–502, https://doi.org/10.1007/s10439-008-9629-2.
[17] R.D. Sumanasinghe, S.H. Bernacki, E.G. Loboa, Osteogenic differentiation of human mesenchymal stem cells in collagen matrices: effect of uniaxial cyclic tensile strain on bone morphogenetic protein (BMP-2) mRNA expression, J. Tissue Eng. 12 (12) (2006) 3459–3465, https://doi.org/10.1089/ten.2006.12.3459.
[18] C.M. Madl, S.C. Heilshorn, H.M. Blau, Bioengineering strategies to accelerate stem cell therapeutics, Nature 557 (7705) (2018) 335–342, https://doi.org/10.1038/s41586-018-0089-z.
[19] N. Huebsch, P.R. Arany, A.S. Mao, D. Shvartsman, O.A. Ali, S.A. Bencherif, J. Rivera-Feliciano, D.J. Mooney, Harnessing traction-mediated manipulation of the cell/matrix interface to control stem-cell fate, Nat. Mater. 9 (6) (2010) 518–526, https://doi.org/10.1038/nmat2732.
[20] K.H. Vining, D.J. Mooney, Mechanical forces direct stem cell behaviour in development and regeneration, Nat. Rev. Mol. Cell Biol. 18 (12) (2017) 728–742, https://doi.org/10.1038/nrm.2017.108.
[21] X. Lin, Y. Shi, Y. Cao, W. Liu, Recent progress in stem cell differentiation directed by material and mechanical cues, Biomed. Mater. 11 (1) (2016), 014109, https://doi.org/10.1088/1748-6041/11/1/014109.
[22] M. Ghasemzadeh-Hasankolaei, J.M. Miranda, C.R. Correia, J.F. Mano, Viscous microcapsules as microbioreactors to study mesenchymal stem/stromal cells osteolineage commitment, Small Methods (2023), 2201503, https://doi.org/10.1002/smtd.202201503.
[23] E. Stavenschi, D.A. Hoey, Pressure-induced mesenchymal stem cell osteogenesis is dependent on intermediate filament remodeling, Faseb. J. 33 (3) (2019) 4178–4187, https://doi.org/10.1096/fj.201801474RR.
[24] E. Stavenschi, M.A. Corrigan, G.P. Johnson, M. Riffault, D.A. Hoey, Physiological cyclic hydrostatic pressure induces osteogenic lineage commitment of human bone marrow stem cells: a systematic study, Stem Cell Res. Ther. 9 (1) (2018) 276, https://doi.org/10.1186/s13287-018-1025-8.
[25] Y. Sun, B. Wan, R. Wang, B. Zhang, P. Luo, D. Wang, J.-J. Nie, D. Chen, X. Wu, Mechanical stimulation on mesenchymal stem cells and surrounding microenvironments in bone regeneration: regulations and applications, Front. Cell Dev. Biol. 10 (2022), 808303, https://doi.org/10.3389/fcell.2022.808303.
[26] C. da Silva Madaleno, J. Jatzlau, P. Knaus, BMP signalling in a mechanical context–Implications for bone biology, Bone 137 (2020), 115416, https://doi.org/10.1016/j.bone.2020.115416.
[27] L. Wang, F. Zheng, R. Song, L. Zhuang, M. Yang, J. Suo, L. Li, Integrins in the regulation of mesenchymal stem cell differentiation by mechanical signals, Stem Cell Rev. Rep. (2021) 1–16, https://doi.org/10.1007/s12015-021-10260-5.
[28] M. Montagner, S. Dupont, Mechanical forces as determinants of disseminated metastatic cell fate, Cells 9 (1) (2020) 250, https://doi.org/10.3390/cells9010250.
[29] L. Polo-Corrales, J. Ramirez-Vick, J.J. Feria-Diaz, Recent advances in biophysical stimulation of MSC for bone regeneration, Indian J. Sci. Technol. 11 (15) (2018) 1–41, https://doi.org/10.17485/ijst/2018/v11i16/121405.
[30] T.M. Maul, D.W. Chew, A. Nieponice, D.A. Vorp, Mechanical stimuli differentially control stem cell behavior: morphology, proliferation, and differentiation, Biomech. Model. Mechanobiol. 10 (6) (2011) 939–953, https://doi.org/10.1007/s10237-010-0285-8.

[31] P. Angele, J. Yoo, C. Smith, J. Mansour, K. Jepsen, M. Nerlich, B. Johnstone, Cyclic hydrostatic pressure enhances the chondrogenic phenotype of human mesenchymal progenitor cells differentiated in vitro, J. Orthop. Res. 21 (3) (2003) 451–457, https://doi.org/10.1016/S0736-0266(02)00230-9.
[32] A.J. Steward, D.J. Kelly, D.R. Wagner, The role of calcium signalling in the chondrogenic response of mesenchymal stem cells to hydrostatic pressure, Eur. Cell. Mater. 28 (2014) 358–371, https://doi.org/10.22203/ecm.v028a25.
[33] C. Huang, R. Ogawa, Effect of hydrostatic pressure on bone regeneration using human mesenchymal stem cells, Tissue Eng. 18 (19–20) (2012) 2106–2113, https://doi.org/10.1089/ten.tea.2012.0064.
[34] Y.H. Zhao, X. Lv, Y.L. Liu, Y. Zhao, Q. Li, Y.J. Chen, M. Zhang, Hydrostatic pressure promotes the proliferation and osteogenic/chondrogenic differentiation of mesenchymal stem cells: the roles of RhoA and Rac1, Stem Cell Res. 14 (3) (2015) 283–296, https://doi.org/10.1016/j.scr.2015.02.006.
[35] J. Klein-Nulend, R. Bacabac, A. Bakker, Mechanical loading and how it affects bone cells: the role of the osteocyte cytoskeleton in maintaining our skeleton, Eur. Cell. Mater. 24 (2) (2012) 279–291, https://doi.org/10.22203/ecm.v024a20.
[36] J.D. Gardinier, C.W. Townend, K.-P. Jen, Q. Wu, R.L. Duncan, L. Wang, In situ permeability measurement of the mammalian lacunar–canalicular system, Bone 46 (4) (2010) 1075–1081, https://doi.org/10.1016/j.bone.2010.01.371.
[37] B. Frey, C. Janko, N. Ebel, S. Meister, E. Schlucker, R. Meyer-Pittroff, R. Fietkau, M. Herrmann, U.S. Gaipl, Cells under pressure-treatment of eukaryotic cells with high hydrostatic pressure, from physiologic aspects to pressure induced cell death, Curr. Med. Chem. 15 (23) (2008) 2329–2336, https://doi.org/10.2174/092986708785909166.
[38] M.J. Barron, C.-J. Tsai, S.W. Donahue, Mechanical stimulation mediates gene expression in MC3T3 osteoblastic cells differently in 2D and 3D environments, J. Biomech. Eng. (2010), https://doi.org/10.1115/1.4001162.
[39] S. Vériter, W. André, N. Aouassar, H.A. Poirel, A. Lafosse, P.-L. Docquier, D. Dufrane, Human adipose-derived mesenchymal stem cells in cell therapy: safety and feasibility in different" hospital exemption" clinical applications, PLoS One 10 (10) (2015), e0139566, https://doi.org/10.1371/journal.pone.0139566.
[40] T. Schubert, D. Xhema, S. Vériter, M. Schubert, C. Behets, C. Delloye, P. Gianello, D. Dufrane, The enhanced performance of bone allografts using osteogenic-differentiated adipose-derived mesenchymal stem cells, Biomaterials 32 (34) (2011) 8880–8891, https://doi.org/10.1016/j.biomaterials.2011.08.009.
[41] W. Mende, R. Götzl, Y. Kubo, T. Pufe, T. Ruhl, J.P. Beier, The role of adipose stem cells in bone regeneration and bone tissue engineering, Cells 10 (5) (2021) 975, https://doi.org/10.3390/cells10050975.
[42] M.H. Moon, S.Y. Kim, Y.J. Kim, S.J. Kim, J.B. Lee, Y.C. Bae, S.M. Sung, J.S. Jung, Human adipose tissue-derived mesenchymal stem cells improve postnatal neovascularization in a mouse model of hindlimb ischemia, Cell. Physiol. Biochem. 17 (5–6) (2006) 279–290, https://doi.org/10.1159/000094140.
[43] S. Tajima, M. Tobita, H. Orbay, H. Hyakusoku, H. Mizuno, Direct and indirect effects of a combination of adipose-derived stem cells and platelet-rich plasma on bone regeneration, Tissue Eng. 21 (5–6) (2015) 895–905, https://doi.org/10.1089/ten.tea.2014.0336.
[44] S. Lendeckel, A. Jödicke, P. Christophis, K. Heidinger, J. Wolff, J.K. Fraser, M. H. Hedrick, L. Berthold, H.-P. Howaldt, Autologous stem cells (adipose) and fibrin glue used to treat widespread traumatic calvarial defects: case report, Maxillofac. Surg. 32 (6) (2004) 370–373, https://doi.org/10.1016/j.jcms.2004.06.002.
[45] G.K. Sándor, V.J. Tuovinen, J. Wolff, M. Patrikoski, J. Jokinen, E. Nieminen, B. Mannerström, O.-P. Lappalainen, R. Seppänen, S. Miettinen, Adipose stem cell tissue–engineered construct used to treat large anterior mandibular defect: a case report and review of the clinical application of good manufacturing practice–level adipose stem cells for bone regeneration, Oral Maxillofac. Surg. 71 (5) (2013) 938–950, https://doi.org/10.1016/j.joms.2012.11.014.
[46] B. Saçak, F. Certel, Z.D. Akdeniz, B. Karademir, F. Ercan, N. Özkan, İ.N. Akpinar, Ö. Çelebiler, Repair of critical size defects using bioactive glass seeded with adipose-derived mesenchymal stem cells, Biomed. Mater. Res. Part B Appl. Biomater. 105 (5) (2017) 1002–1008, https://doi.org/10.1002/jbm.b.33634.
[47] C.R. Correia, M. Ghasemzadeh-Hasankolaei, J.F. Mano, Cell encapsulation in liquified compartments: protocol optimization and challenges, PLoS One 14 (6) (2019), https://doi.org/10.1371/journal.pone.0218045.
[48] C.R. Correia, R.L. Reis, J.o.F. Mano, Multilayered hierarchical capsules providing cell adhesion sites, Biomacromolecules 14 (3) (2013) 743–751, https://doi.org/10.1021/bm301833z.
[49] C.R. Correia, R.P. Pirraco, M.T. Cerqueira, A.P. Marques, R.L. Reis, J.F. Mano, Semipermeable capsules wrapping a multifunctional and self-regulated co-culture microenvironment for osteogenic differentiation, Sci. Rep. 6 (2016), 21883, https://doi.org/10.1038/srep21883.
[50] C.R. Correia, T.C. Santos, R.P. Pirraco, M.T. Cerqueira, A.P. Marques, R.L. Reis, J. F. Mano, In vivo osteogenic differentiation of stem cells inside compartmentalized capsules loaded with co-cultured endothelial cells, Acta Biomater. 53 (2017) 483–494, https://doi.org/10.1016/j.actbio.2017.02.007.
[51] C.S. Oliveira, S. Nadine, M.C. Gomes, C.R. Correia, J.F. Mano, Bioengineering the human bone marrow microenvironment in liquefied compartments: a promising approach for the recapitulation of osteovascular niches, Acta Biomater. 149 (2022) 167–178, https://doi.org/10.1016/j.actbio.2022.07.001.
[52] S. Nadine, S.G. Patrício, C.R. Correia, J.F. Mano, Dynamic microfactories co-encapsulating osteoblastic and adipose-derived stromal cells for the biofabrication of bone units, Biofabrication 12 (1) (2019), 015005, https://doi.org/10.1088/1758-5090/ab3e16.
[53] V.M. Gaspar, P. Lavrador, J. Borges, M.B. Oliveira, J.F. Mano, Advanced bottom-up engineering of living architectures, Adv. Mater. 32 (6) (2020), 1903975, https://doi.org/10.1002/adma.201903975.
[54] M.V. Monteiro, M. Rocha, V.M. Gaspar, J.F. Mano, Programmable living units for emulating pancreatic tumor-stroma interplay, Adv. Healthcare Mater. 11 (13) (2022), 2102574, https://doi.org/10.1002/adhm.202102574.
[55] M.M. Maciel, T.R. Correia, V.M. Gaspar, J.M. Rodrigues, I.S. Choi, J.F. Mano, Partial coated stem cells with bioinspired silica as new generation of cellular hybrid materials, Adv. Funct. Mater. 31 (29) (2021), 2009619, https://doi.org/10.1002/adfm.202009619.
[56] A. Mahara, N. Morimoto, T. Sakuma, T. Fujisato, T. Yamaoka, Complete cell killing by applying high hydrostatic pressure for acellular vascular graft preparation, BioMed Res. Int. 2014 (2014), 379607, https://doi.org/10.1155/2014/379607.
[57] K.J. Takano, T. Takano, Y. Yamanouchi, T. Satou, Pressure-induced apoptosis in human lymphoblasts, Exp. Cell Res. 235 (1) (1997) 155–160, https://doi.org/10.1006/excr.1997.3666.
[58] I. Adkins, N. Hradilova, O. Palata, L. Sadilkova, L. Palova-Jelinkova, R. Spisek, High hydrostatic pressure in cancer immunotherapy and biomedicine, Biotechnol. Adv. 36 (3) (2018) 577–582, https://doi.org/10.1016/j.biotechadv.2018.01.015.
[59] T.M. Le, N. Morimoto, N.T.M. Ly, T. Mitsui, S.C. Notodihardjo, M.C. Munisso, N. Kakudo, H. Moriyama, T. Yamaoka, K. Kusumoto, Hydrostatic pressure can induce apoptosis of the skin, Sci. Rep. 10 (1) (2020) 1–16, https://doi.org/10.1038/s41598-020-74695-5.
[60] I.M. Bjørge, B.M. de Sousa, S.G. Patrício, A.S. Silva, L.P. Nogueira, L.c.F. Santos, S. I. Vieira, H.v.J. Haugen, C.R. Correia, J.o.F. Mano, Bioengineered hierarchical bonelike compartmentalized microconstructs using nanogrooved microdiscs, ACS Appl. Mater. Interfaces (2022), https://doi.org/10.1021/acsami.2c01161.
[61] J.M. Silva, A.R.C. Duarte, S.G. Caridade, C. Picart, R.L. Reis, J.F. Mano, Tailored freestanding multilayered membranes based on chitosan and alginate, Biomacromolecules 15 (10) (2014) 3817–3826, https://doi.org/10.1021/bm501156v.
[62] W. Zhang, S. Zhao, W. Rao, J. Snyder, J.K. Choi, J. Wang, I.A. Khan, N.B. Saleh, P. J. Mohler, J. Yu, A novel core–shell microcapsule for encapsulation and 3D culture of embryonic stem cells, Mater. Chem. B 1 (7) (2013) 1002–1009, https://doi.org/10.1039/C2TB00058J.
[63] Y. Li, J. Zhou, X. Yang, Y. Jiang, J. Gui, Intermittent hydrostatic pressure maintains and enhances the chondrogenic differentiation of cartilage progenitor cells cultivated in alginate beads, Dev. Growth Differ. 58 (2) (2016) 180–193, https://doi.org/10.1111/dgd.12261.
[64] P. Aprile, D.J. Kelly, Hydrostatic pressure regulates the volume, aggregation and chondrogenic differentiation of bone marrow derived stromal cells, Front. Bioeng. Biotechnol. 8 (2021), 619914, https://doi.org/10.3389/fbioe.2020.619914.
[65] H. Huang, C. Dai, H. Shen, M. Gu, Y. Wang, J. Liu, L. Chen, L. Sun, Recent advances on the model, measurement technique, and application of single cell mechanics, Int. J. Mol. Sci. 21 (17) (2020) 6248, https://doi.org/10.3390/ijms21176248.
[66] H.C. Crenshaw, J.A. Allen, V. Skeen, A. Harris, E. Salmon, Hydrostatic pressure has different effects on the assembly of tubulin, actin, myosin II, vinculin, talin, vimentin, and cytokeratin in mammalian tissue cells, Exp. Cell Res. 227 (2) (1996) 285–297, https://doi.org/10.1006/excr.1996.0278.
[67] R.G. Wilson Jr., J.E. Trogadis, S. Zimmerman, A.M. Zimmerman, Hydrostatic pressure induced changes in the cytoarchitecture of pheochromocytoma (PC-12) cells, Cell Biol. Int. 25 (7) (2001) 649–666, https://doi.org/10.1006/cbir.2000.0692.
[68] K. Okamoto, T.M. Watanabe, M. Horie, M. Nishiyama, Y. Harada, H. Fujita, Pressure-induced changes on the morphology and gene expression in mammalian cells, Biol. Open 10 (7) (2021), bio058544, https://doi.org/10.1242/bio.058544.
[69] S.-H. Park, W.Y. Sim, B.-H. Min, S.S. Yang, A. Khademhosseini, D.L. Kaplan, Chip-based comparison of the osteogenesis of human bone marrow-and adipose tissue-derived mesenchymal stem cells under mechanical stimulation, PLoS One (2012), https://doi.org/10.1371/journal.pone.0046689.
[70] R.L. Smith, S. Rusk, B. Ellison, P. Wessells, K. Tsuchiya, D. Carter, W. Caler, L. Sandell, D. Schurman, In vitro stimulation of articular chondrocyte mRNA and extracellular matrix synthesis by hydrostatic pressure, J. Orthop. Res. 14 (1) (1996) 53–60, https://doi.org/10.1002/jor.1100140110.
[71] R.L. Smith, J. Lin, M. Trindade, J. Shida, G. Kajiyama, T. Vu, A. Hoffman, M. Van Der Meulen, S. Goodman, D. Schurman, Time-dependent effects of intermittent hydrostatic pressure on articular chondrocyte type II collagen and aggrecan mRNA expression, J. Rehabil. Res. Dev. 37 (2000) 153–161. https://pubmed.ncbi.nlm.nih.gov/10850821.
[72] R.M. Ezzell, W.H. Goldmann, N. Wang, N. Parasharama, D.E. Ingber, Vinculin promotes cell spreading by mechanically coupling integrins to the cytoskeleton, Exp. Cell Res. 231 (1) (1997) 14–26, https://doi.org/10.1006/excr.1996.3451.
[73] E. Barcelona-Estaje, M.J. Dalby, M. Cantini, M. Salmeron-Sanchez, You talking to me? Cadherin and integrin crosstalk in biomaterial design, Adv. Healthcare Mater. 10 (6) (2021), 2002048, https://doi.org/10.1002/adhm.202002048.
[74] R. Zohar, S. Cheifetz, C.A. McCulloch, J. Sodek, Analysis of intracellular osteopontin as a marker of osteoblastic cell differentiation and mesenchymal cell migration, Eur. J. Oral Sci. 106 (S1) (1998) 401–407, https://doi.org/10.1111/j.1600-0722.1998.tb02206.x.
[75] M. Morinobu, M. Ishijima, S.R. Rittling, K. Tsuji, H. Yamamoto, A. Nifuji, D. T. Denhardt, M. Noda, Osteopontin expression in osteoblasts and osteocytes during bone formation under mechanical stress in the calvarial suture in vivo, J. Bone Miner. Res. 18 (9) (2003) 1706–1715, https://doi.org/10.1359/jbmr.2003.18.9.1706.
[76] J. Chen, C. Li, L. Chen, The role of microvesicles derived from mesenchymal stem cells in lung diseases, BioMed Res. Int. 2015 (2015), https://doi.org/10.1155/2015/985814.
[77] A.C.C. de Paula, A.A.C. Zonari, T.M.d.M. Martins, S. Novikoff, A.R.P. da Silva, V. M. Correlo, R.L. Reis, D.A. Gomes, A.M. Goes, Human serum is a suitable

supplement for the osteogenic differentiation of human adipose-derived stem cells seeded on poly-3-hydroxibutyrate-co-3-hydroxyvalerate scaffolds, Tissue Eng. 19 (1–2) (2013) 277–289, https://doi.org/10.1089/ten.tea.2012.0189.
[78] K.S. Katti, A.H. Ambre, S. Payne, D.R. Katti, Vesicular delivery of crystalline calcium minerals to ECM in biomineralized nanoclay composites, Mater. Res. Express 2 (4) (2015), 045401, https://doi.org/10.1088/2053-1591/2/4/045401.
[79] J. Mahamid, A. Sharir, D. Gur, E. Zelzer, L. Addadi, S. Weiner, Bone mineralization proceeds through intracellular calcium phosphate loaded vesicles: a cryo-electron microscopy study, J. Struct. Biol. 174 (3) (2011) 527–535, https://doi.org/10.1016/j.jsb.2011.03.014.
[80] L. Luo, N.C. Foster, K.L. Man, M. Brunet, D.A. Hoey, S.C. Cox, S.J. Kimber, A.J. El Haj, Hydrostatic pressure promotes chondrogenic differentiation and microvesicle release from human embryonic and bone marrow stem cells, Biotechnol. J. 17 (4) (2022), 2100401, https://doi.org/10.1002/biot.202100401.
[81] S. Trivedi, K. Srivastava, A. Gupta, T.S. Saluja, S. Kumar, D. Mehrotra, S.K. Singh, A quantitative method to determine osteogenic differentiation aptness of scaffold, J. Oral Biol. 10 (2) (2020) 158–160, https://doi.org/10.1016/j.jobcr.2020.04.006.
[82] A. Steward, S. Thorpe, T. Vinardell, C. Buckley, D. Wagner, D. Kelly, Cell–matrix interactions regulate mesenchymal stem cell response to hydrostatic pressure, Acta Biomater. 8 (6) (2012) 2153–2159, https://doi.org/10.1016/j.actbio.2012.03.016.
[83] H.-X. Shen, J.-Z. Liu, X.-Q. Yan, H.-N. Yang, S.-Q. Hu, X.-L. Yan, T. Xu, A.J. El Haj, Y. Yang, L.-X. Lü, Hydrostatic pressure stimulates the osteogenesis and angiogenesis of MSCs/HUVECs co-culture on porous PLGA scaffolds, Colloids Surf., B 213 (2022), 112419, https://doi.org/10.1016/j.colsurfb.2022.112419.
[84] X. Wang, W. Song, N. Kawazoe, G. Chen, The osteogenic differentiation of mesenchymal stem cells by controlled cell–cell interaction on micropatterned surfaces, J. Biomed. Mater. Res., Part A 101 (12) (2013) 3388–3395, https://doi.org/10.1002/jbm.a.34645.
[85] F. Jiao, J. Xu, Y. Zhao, C. Ye, Q. Sun, C. Liu, B. Huo, Synergistic effects of fluid shear stress and adhesion morphology on the apoptosis and osteogenesis of mesenchymal stem cells, J. Biomed. Mater. Res., Part A (2022), https://doi.org/10.1002/jbm.a.37413.
[86] N. Datta, Q.P. Pham, U. Sharma, V.I. Sikavitsas, J.A. Jansen, A.G. Mikos, In vitro generated extracellular matrix and fluid shear stress synergistically enhance 3D osteoblastic differentiation, Proc. Natl. Acad. Sci. U.S.A. 103 (8) (2006) 2488–2493, https://doi.org/10.1073/pnas.0505661103.
[87] J. He, D. You, Q. Li, J. Wang, S. Ding, X. He, H. Zheng, Z. Ji, X. Wang, X. Ye, Osteogenesis-inducing chemical cues enhance the mechanosensitivity of human mesenchymal stem cells for osteogenic differentiation on a microtopographically patterned surface, Adv. Sci. (2022), 2200053, https://doi.org/10.1002/advs.202200053.
[88] G. Yourek, S.M. McCormick, J.J. Mao, G.C. Reilly, Shear stress induces osteogenic differentiation of human mesenchymal stem cells, Regen. Med. 5 (5) (2010) 713–724, https://doi.org/10.2217/rme.10.60.